Karbala International Journal of Modern Science

Manuscript 3405

Computational Design of Potent siRNA for BRAF Oncogene Silencing for Enhancing Cancer Therapy

Muhammad Hermawan Widyananda

Ricadonna Raissa

Computational Design of Potent siRNA for BRAF Oncogene Silencing for Enhancing Cancer Therapy

Abstract

The discovery of oncogenic BRAF mutations has prompted the development of inhibitors, yet resistance remains widespread. A more effective strategy involves targeting BRAF mRNA with siRNA to overcome resistance to BRAF inhibitors. This study aims to design potent siRNA for BRAF oncogene silencing using a computational approach. The full coding sequence of BRAF was retrieved from the NCBI database and potential siRNAs were predicted using the Ui-Tei, Reynolds, and Amarzguioui rules. Identified siRNAs were further analyzed using various prediction systems and parameters, including their interaction with the hAgo2 protein. The results identified that seven siRNAs (siRNA 23, siRNA 24, siRNA 26, siRNA 34, siRNA 37, and siRNA 38) with high potential for targeting BRAF mRNA. These siRNAs demonstrated a GC content above 30%, a high prediction score, a low probabilities of self-folding, and strong binding affinities to the target mRNA. Among these, three siRNAs (siRNA 28, siRNA 34, and siRNA 38) exhibited the most negative binding energy values, namely -352.88, -353.48, and -356.46 kcal/mol, respectively. Structural analyses of hAgo2, siRNAs, and their interactions revealed that siRNA 34 (5'-UUCCAAAUGCAUAUACAUCUG-3') and siRNA 38 (5'-UUGUUGAUGUUUGAAUAAGGU-3') had the highest potential as BRAF silencers. The siRNA 34 and siRNA 38 exhibited the highest potential for BRAF silencing. This study provides a comprehensive computational approach for designing siRNAs, aiming to enhance the effectiveness of siRNA-based therapeutic strategies.

Keywords

BRAF, cancer, hAgo2, siRNA, oncogene

RESEARCH PAPER

Computational Design of Potent siRNA for BRAF Oncogene Silencing for Enhancing Cancer Therapy

Muhammad H. Widyananda [a], Ricadonna Raissa [b,*]

[a] Department of Biology, Faculty of Mathematics and Natural Sciences, Universitas Brawijaya, Malang, Indonesia
[b] Department of Pharmacology, Faculty of Veterinary Medicine, Universitas Brawijaya, Malang, Indonesia

Abstract

The discovery of oncogenic BRAF mutations has prompted the development of inhibitors, yet resistance remains widespread. A more effective strategy involves targeting BRAF mRNA with siRNA to overcome resistance to BRAF inhibitors. This study aims to design potent siRNA for BRAF oncogene silencing using a computational approach. The full coding sequence of BRAF was retrieved from the NCBI database and potential siRNAs were predicted using the Ui-Tei, Reynolds, and Amarzguioui rules. Identified siRNAs were further analyzed using various prediction systems and parameters, including their interaction with the hAgo2 protein. The results identified that seven siRNAs (siRNA 23, siRNA 24, siRNA 26, siRNA 34, siRNA 37, and siRNA 38) with high potential for targeting BRAF mRNA. These siRNAs demonstrated a GC content above 30 %, high prediction score, low probabilities of self-folding, and strong binding affinities to the target mRNA. Among these, three siRNAs (siRNA 28, siRNA 34, and siRNA 38) exhibited the most negative binding energy values, namely −352.88, −353.48, and −356.46 kcal/mol, respectively. Structural analyses of hAgo2, siRNAs, and their interactions revealed that siRNA 34 (5′-UUCCAAAUGCAUAUACAUCUG-3′) and siRNA 38 (5′-UUGUUGAUGUUUGAAUAAGGU-3′) had the highest potential as BRAF silencers. The siRNA 34 and siRNA 38 exhibited the highest potential for BRAF silencing. This study provides a comprehensive computational approach for designing siRNAs, aiming to enhance the effectiveness of siRNA-based therapeutic strategies.

Keywords: BRAF, Cancer, hAgo2, siRNA, Oncogene

1. Introduction

In mammalian cells, the RAF protein family plays a crucial role in regulating cell proliferation, differentiation, and survival [1]. The RAF family consists of three conserved domains known as conserved regions 1, 2, and 3 (CR1, CR2, CR3). These domains have distinct functions: CR1 serves as a self-regulatory domain for RAS GTP-binding, CR2 functions as a serine-rich hinge region, and CR3 acts as a catalytic domain for serine/threonine protein kinase, responsible for phosphorylating a consensus sequence on protein substrates [2].

The RAF family comprises three proteins: ARAF, BRAF, and CRAF. Among these, BRAF mutations are the most common alterations in the RAF kinase family, frequently observed in various cancer types, including nearly 60 % of melanomas, 60 % of thyroid cancers, 15 % of colorectal cancers, and 5−8 % of non-small cell lung cancers (NSCLCs). Mutations in BRAF lead to over activity of the ERK signaling pathway resulting in uncontrolled cell proliferation [3]. Therefore, research to develop effective BRAF inhibitors is progressing rapidly.

The discovery of oncogenic BRAF mutations has driven the development of inhibitors targeting BRAF [4]. Vemurafenib and Dabrafenib are small molecule inhibitors that specifically target BRAF. Both compounds act as ATP inhibitors that bind to the ATP binding domain of BRAF protein [5]. In addition small molecules, antibody-based BRAF inhibitors have also been developed to specifically inactivate BRAF [6]. However, resistance to BRAF inhibitors is a significant challenge. Previous clinical research involving 132 samples reported that 58 % of patients experienced resistance to BRAF inhibitor [7]. Resistance

Received 23 January 2025; revised 11 April 2025; accepted 15 April 2025.
Available online 8 May 2025

* Corresponding author.
E-mail address: ricadonnaraissa@ub.ac.id (R. Raissa).

https://doi.org/10.33640/2405-609X.3405

mechanisms include gene amplification and mutation mechanisms in BRAF. The amplification of the BRAF gene resulted in a substantial increase in BRAF protein expression, leading to the reactivation of ERK in the presence of BRAF inhibitors. Additionally, inhibitor molecules can also induce mutation in BRAF, making the protein resistant to inhibitors [8]. Due to the emergence of various cases of BRAF resistance, a more effective strategy BRAF inhibition is needed. Targeting BRAF at the mRNA level using siRNA offers a promising alternative.

The siRNA-based cancer therapy method has high prospects as an anticancer alternative because it directly silences the expression of specific genes [9]. One of siRNA advantages is the ability to overcome resistance to small-molecule inhibitors and monoclonal antibody inhibitors [10]. For example, previous research demonstrated that siRNA targeting the HER3 protein effectively overcomes resistance to small-molecule HER3 inhibitors. Another study stated that siRNA targeting MDM2 induces apoptosis in chemotherapy-resistant non-small cell lung cancer [11]. These findings highlight the effectiveness of siRNA as a promising approach to address designing siRNAs targeting oncogenes frequently associated with drug resistance mechanisms is an urgent necessity.

The increasing resistance of cancer to drugs emphasizes the critical requirement for innovative therapeutic approaches. Our research addresses this challenge by employing computational design to enhance cancer therapy. We concentrate on the precise development of powerful siRNA molecules to selectively silence the BRAF oncogene. The following sections will detail the computational design methodology and the rationale for selecting specific siRNA candidates.

2. Methods

2.1. BRAF sequence retrieval

The complete coding sequence (CDS) of BRAF oncogene (NM_001378474.1) were obtained from NCBI (https://www.ncbi.nlm.nih.gov/) with RefSeq as the Source database. This sequence was obtained from chromosome 7q34 from humans suffering from thyroid cancer [12]. The CDS sequence was saved in fasta format. The BRAF sequence obtained was continued to the next stages as shown in the flowchart in Fig. 1.

2.2. siRNA sequence prediction

The sequences of the siRNA targeting the BRAF mRNA were predicted using siDirect 2.1 web server (https://sidirect2.rnai.jp/) using Human (Homo sapiens) transcript RefSeq release 220 as the reference. siRNA prediction uses a combination of the Ui-Tei + Reynolds + Amarzguioui algorithm [13]. Sequences that have a melting temperature of 20–60 °C were chosen because they have good silencing activity.

2.3. Validation and off-target analysis of predicted siRNA

Validation of siRNA obtained from siDirect 2.1 was carried out using siExplorer (http://rna.chem.t.u-tokyo.ac.jp/cgi/siexplorer.htm) [14]. And OligoWalk (https://rna.urmc.rochester.edu/cgi-bin/server_exe/oligowalk/oligowalk_form.cgi) [15]. Prediction of siRNA inhibition ability was performed using siPRED (http://predictor.nchu.edu.tw/siPRED/) [16]. Off-targets of each siRNA were analyzed using BLAST NCBI.

2.4. siRNAs folding probability analysis

The secondary structure and the free energy of folding of the designed siRNAs guide strands were predicted using default parameters in the MaxExpect webserver (https://rna.urmc.rochester.edu/RNAstructureWeb/Servers/MaxExpect/MaxExpect.html) [17]. The low energy value implies more possible folding and the high energy value implies less possible folding, and thus the siRNA guide strands showing high energy will be the more suitable candidates.

2.5. siRNAs-mRNA binding analysis

The interaction binding energy of siRNA with target mRNA was predicted using DuplexFold web server (https://rna.urmc.rochester.edu/RNAstructureWeb/Servers/DuplexFold/DuplexFold.html) [18]. The simulation was carried out at human physiological temperature (310.15 K). A low binding energy value indicates a stable interaction and is an important point for siRNA efficacy.

2.6. Heat capacity and melting temperature calculation of siRNA-mRNA

The DINAMelt web server (http://www.unafold.org/hybrid2.php) was employed to predict the temperature-dependent ensemble heat capacity (Cp), considering the melting temperature at the endpoint (Tm (Cp)) [19]. Additionally, the server was used to calculate the melting temperature at one-half concentration of double-stranded molecules (Tm (Conc)) for the mRNA–siRNA complex.

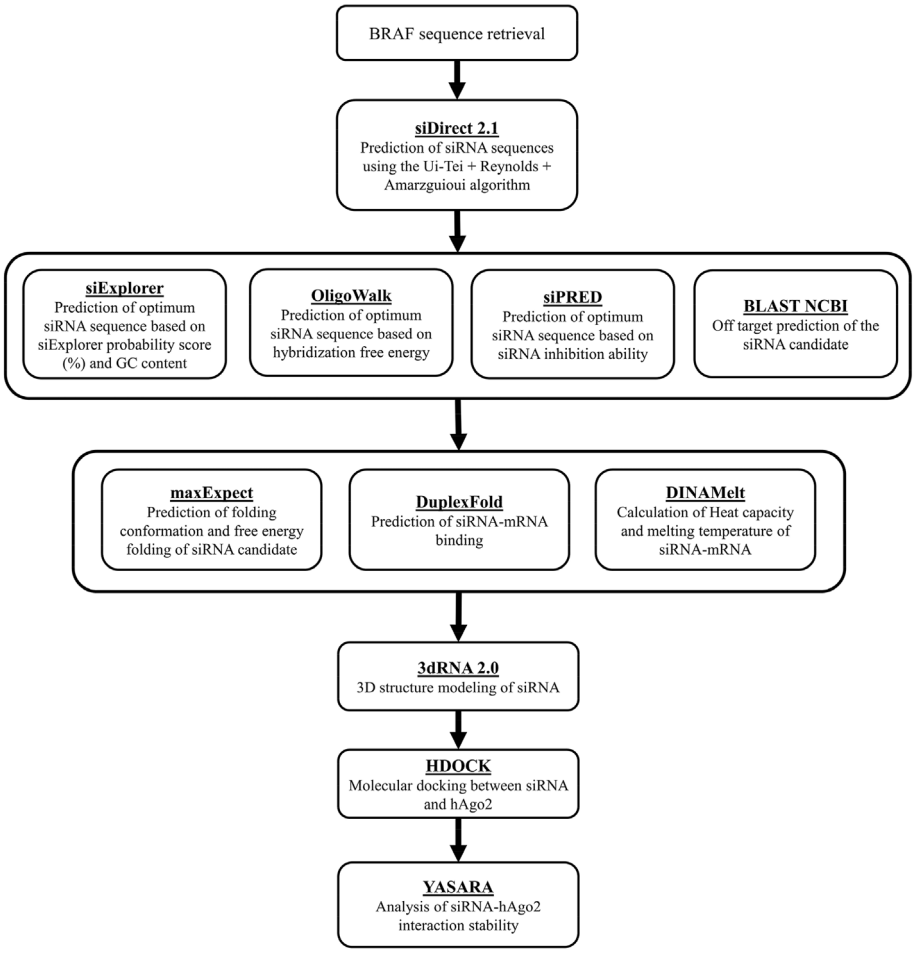

Fig. 1. The flowchart describes the methodology used in the current study along with the respective tool/web server.

2.7. Molecular docking

The 3D structure of siRNA was modeled using the 3dRNA 2.0 web server with Bi-residue as loop building method (http://biophy.hust.edu.cn/new/3dRNA/) [20]. The model used is the model that has the lowest 3dRNA score value. The 3D structure of siRNA was minimized using AMBER with ff14SB force field. The 3D structure of human Argonaute 2 protein (hAgo2) was obtained from the RCSB PDB database (https://www.rcsb.org/) with ID 5JS1 and prepared by removing contaminant molecules using Biovia Discovery Studio 2019 software. Molecular docking between siRNA and hAgo2 was carried out using the HDOCK web server (http://hdock.phys.hust.edu.cn/) [21]. Docking results were visualized using Biovia Discovery Studio 2019.

2.8. Molecular dynamic (MD) simulation

Molecular dynamics simulations were conducted using Yet Another Scientific Artificial Reality Application (YASARA v23.4.25) software with AMBER 14 as a force filed [22]. The system is arranged in the form of a cube filled with water with a density of 997 kg/m^3 and 0.09 % salt. The system conditions are adjusted to human physiological conditions, namely temperature 37 °C, pH 7.4, and pressure 1 atm. The simulation was carried out for 50 ns with autosave enabled every 25 ps. Running the simulation using the md_run program and analyzing the simulation results using md_analyze and md_analyzeres.

3. Results

3.1. Identification and screening of siRNAs sequence targeting BRAF mRNA

The identification of potential siRNAs targeting BRAF mRNA was performed using the siDirect 2.1 webserver, which applies the Ui-Tei, Amarzguioui, and Reynolds rules to enhance the accuracy of siRNA predictions. The analysis identified 39 potential siRNAs targeting various regions of the BRAF mRNA. From these, siRNAs with the most favorable

melting temperature (Tm) values were selected. Among the 39 siRNAs, seven candidates (siRNA 23, siRNA 24, siRNA 26, siRNA 28, siRNA 34, siRNA 37, and siRNA 38) were predicted to have the highest potential, as they exhibited Tm values above 20 °C (see Supplementary Materials, Table 1 (https://kijoms.uokerbala.edu.iq/cgi/editor.cgi?article=3405&window=additional_files&context=home)).

3.2. Validation of siRNAs sequence

The seven potential siRNAs were validated using various parameters, including GC content, free energy, siRNA score, and off-target potential. All seven siRNAs exhibited a GC content above 30 % and showed no indication of off-target effects (see Supplementary Materials, Table 2 (https://kijoms.uokerbala.edu.iq/cgi/editor.cgi?article=3405&window=additional_files&context=home)). The OligoWalk and siExplorer scores were used to predict the likelihood of each sequence being an optimal siRNA, with OligoWalk scores ranging from 0.59 to 0.85 and siExplorer scores between 62.31 % and 76.7 %. The siPred inhibition values, which estimate the ability of siRNAs to inhibit gene expression, ranged from 66.88–81.03 % for the seven candidates (Table 1). Overall, these results suggest that the seven siRNA sequences are highly likely to be effective in targeting BRAF mRNA.

3.3. Potential siRNA secondary structure prediction

This study predicted the potential for siRNA to form secondary structures. The predicted secondary structure conformations and their corresponding free energy folding values are presented in Fig. 2. A positive free energy folding value suggests the likelihood of secondary structure formation. The formation of secondary structures is crucial for preventing siRNA degradation.

3.4. mRNA-siRNA interaction prediction

The potential interactions between candidate siRNAs and target mRNAs were predicted using DuplexFold. The results, including free binding energy values and interaction conformations, are presented in Fig. 3. The free binding energy values ranged from −29.5 to −33.8 kcal/mol, with lower values indicating more stable interactions.

3.5. Heat capacity analysis of potential siRNAs

The heat capacity of the potential siRNAs was evaluated using the endpoint temperature (Tm(Cp))

Table 1. siRNA validation using various parameters and system prediction.

siRNA name	siRNA guide strand (5′→3′)	GC%	Free energy folding (kcal/mol)	Free energy binding (Kcal/mol)	Tm (Cp) (°C)	Tm (Conc) (°C)	siPred Inhibition (%)	Oligo Walk Probability score	siExplorer probability score (%)	Off target
siRNA 23	UUUCUGUAAG GCUUUCACGUU	42.1	1.7	−33.2	78.4	77.9	77.53	0.82	62.68	No
siRNA 24	AUGAAGAUGA CUUCCUUUCUC	42.1	1.8	−33.8	75.3	76.1	79.20	0.61	66.88	No
siRNA 26	UCACAUUCAA CAUUUUCACUG	31.4	1.8	−31.1	73.7	72.9	79.82	0.74	66.98	No
siRNA 28	AUUCACAUGU CGUGUUUUCCU	36.8	1.8	−33.6	76.6	77.6	66.88	0.67	62.31	No
siRNA 34	UUCCAAAUGC AUAUACAUCUG	36.8	1.7	−32	72.8	72.5	79.91	0.59	76.7	No
siRNA 37	UGUUGAUGUU UGAAUAAGGUA	31.5	1.6	−30.2	72	70.9	81.03	0.85	69.29	No
siRNA 38	UUGUUGAUGU UUGAAUAAGGU	31.5	1.7	−29.5	71.6	70.5	79.22	0.84	69.29	No

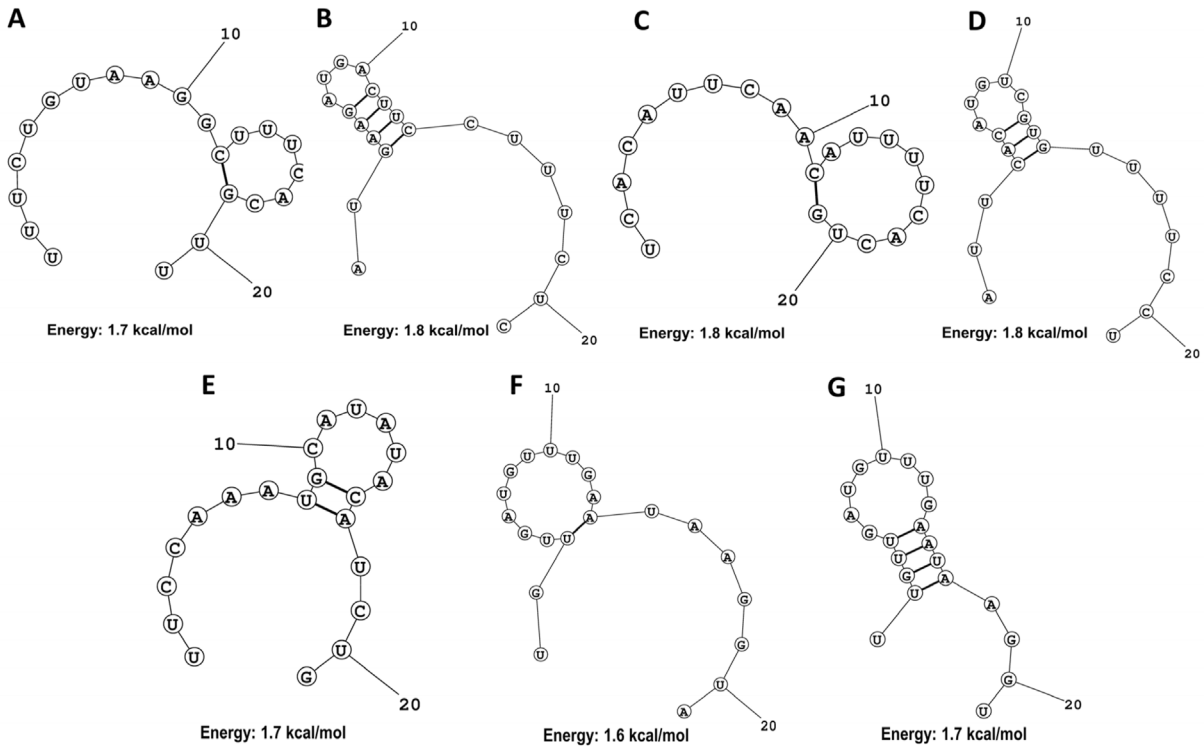

Fig. 2. Self-folding probability and folding energy of potential siRNA guide strand. A) siRNA 23, B) siRNA 24, siRNA 26, siRNA 28, siRNA 34, siRNA 37, siRNA 38.

and the melting temperature at half-concentration of the mRNA-siRNA complex (Tm(Conc)). High Tm(Cp) and Tm(Conc) values indicate a greater likelihood of effective siRNA targeting of the mRNA. In this study, the Tm(Cp) values of the seven potential siRNAs ranged from 70.5 °C to 77.9 °C (Fig. 4A), while the Tm(Conc) values were within the range of 71.6 °C–78.4 °C (Fig. 4B).

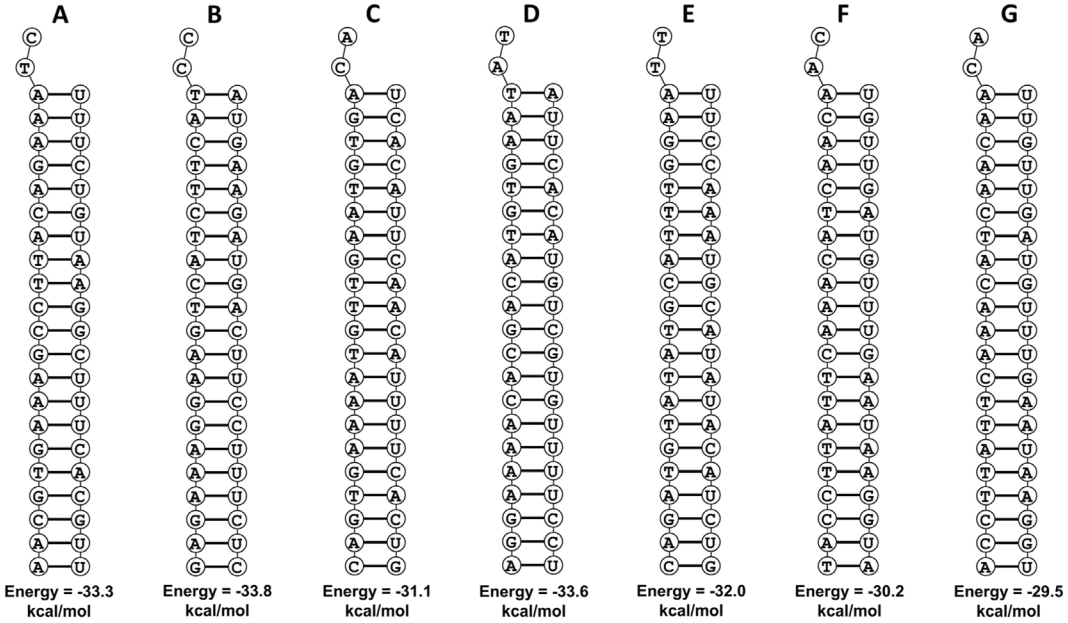

Fig. 3. Probability binding conformations of the siRNA guide strand with the target mRNA and their binding energy values. A) siRNA 23, B) siRNA 24, siRNA 26, siRNA 28, siRNA 34, siRNA 37, siRNA 38.

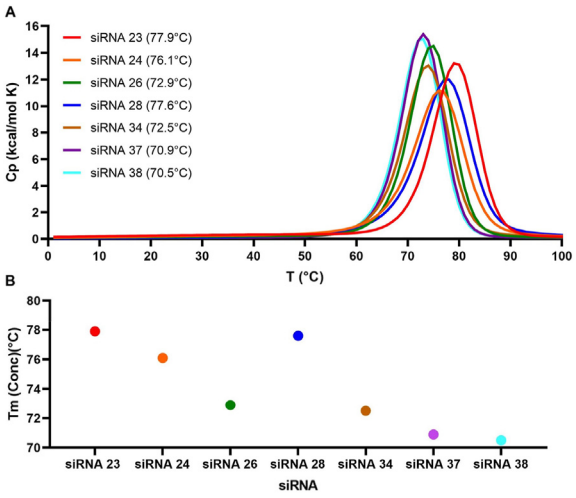

Fig. 4. Heat capacity of the mRNA-siRNAs. A) melting temperature at the endpoint [Tm (Cp)]. B) Melting temperature at one-half concentration of double-stranded molecules [Tm (Conc)].

3.6. Molecular interaction of hAgo2 and potential siRNAs

The interaction between potential siRNAs and hAgo2 is critical, as it underpins the mechanism of recognition and binding to target mRNA. The visualization of the hAgo2-siRNA interaction is presented in Fig. 5. Docking analysis revealed that three complexes exhibited the most stable binding energy values. Specifically, hAgo2-siRNA28 (−352.88 kcal/mol) formed interactions with 18 residues, hAgo2-siRNA34 (−353.48 kcal/mol) formed interactions with 20 residues, and hAgo2-siRNA38 (−356.46 kcal/mol) formed interactions with 20 residues (see supplementary materials, Table 3 (https://kijoms.uokerbala.edu.iq/cgi/editor.cgi?article=3405&window=additional_files&context=home)).

3.7. hAgo2-siRNA complexes dynamic

The three complexes exhibiting the most stable interactions from the docking results (siRNA28-hAgo2, siRNA34-hAgo2, and siRNA38-hAgo2) were further analyzed using molecular dynamics simulations to examine the dynamics of their interactions. The molecular dynamics analysis revealed that the backbone RMSD and radius of gyration values were highest for the hAgo2-siRNA28 complex, suggesting that the hAgo2

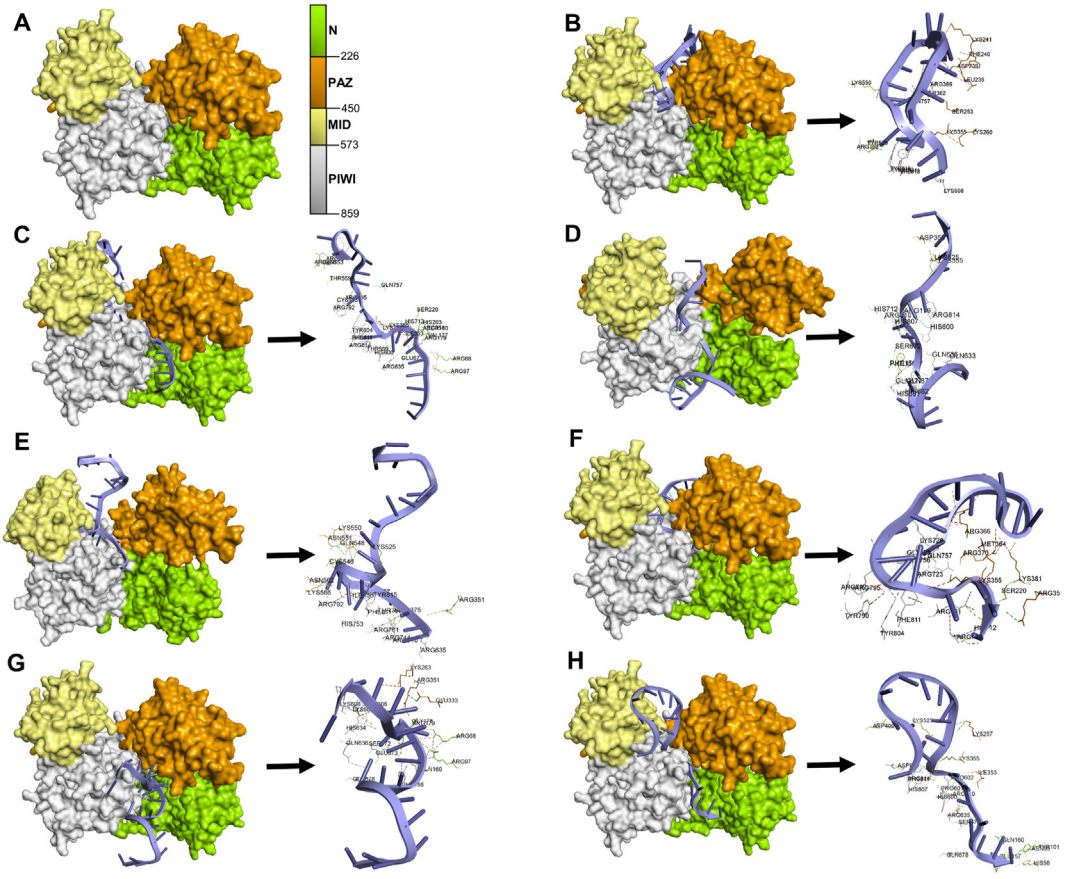

Fig. 5. Molecular interaction between hAgo2 and siRNAs. A) hAgo2 protein structure, B) hAgo2-siRNA 23, C) hAgo2-siRNA 24, D) hAgo2-siRNA 26, E) hAgo2-siRNA 28, F) hAgo2-siRNA 34, G) hAgo2-siRNA 37, H) hAgo2-siRNA 38.

protein structure became less stable after binding to siRNA 28 (Fig. 6A and C). However, the number of hydrogen bonds in all complexes showed minimal fluctuations, indicating no evidence of hAgo2 protein degradation despite the observed structural instability after binding to siRNA 28 (Fig. 6D).

The hAgo2-siRNA 28 complex exhibited the highest RMSD value, suggesting that siRNA28 was less stable when interacting with hAgo2 (Fig. 6B). Additionally, the DCCM analysis of the hAgo2 protein and hAgo2-siRNA complexes showed a trend comparable to that of the control, indicating minimal conformational changes in the hAgo2-siRNA complexes (Fig. 6E–H).

Analyzing the movement of each amino acid in hAgo2 and each nitrogen base in siRNA is essential for a deeper understanding of structural stability. Most residues exhibited RMSF values below 3 Å, indicating that the hAgo2 protein structure remains relatively stable. In contrast, the RMSF values for the nitrogen bases comprising siRNA were higher, particularly for siRNA 28 and siRNA 38, suggesting significant structural flexibility of the siRNA upon binding to hAgo2 (Fig. 7).

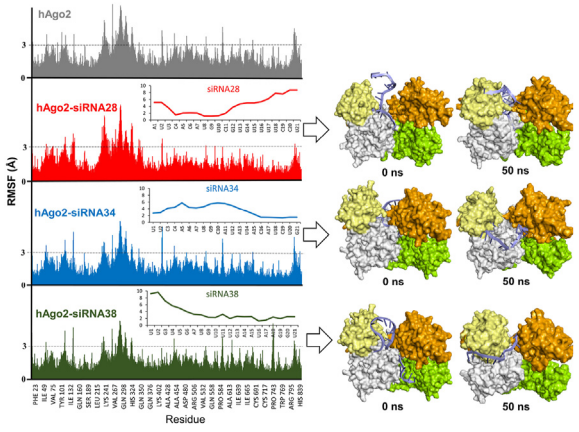

Fig. 7. Root mean square fluctuation of hAgo2-siRNA complex and siRNAs alone and the conformational change of siRNAs before and after simulation.

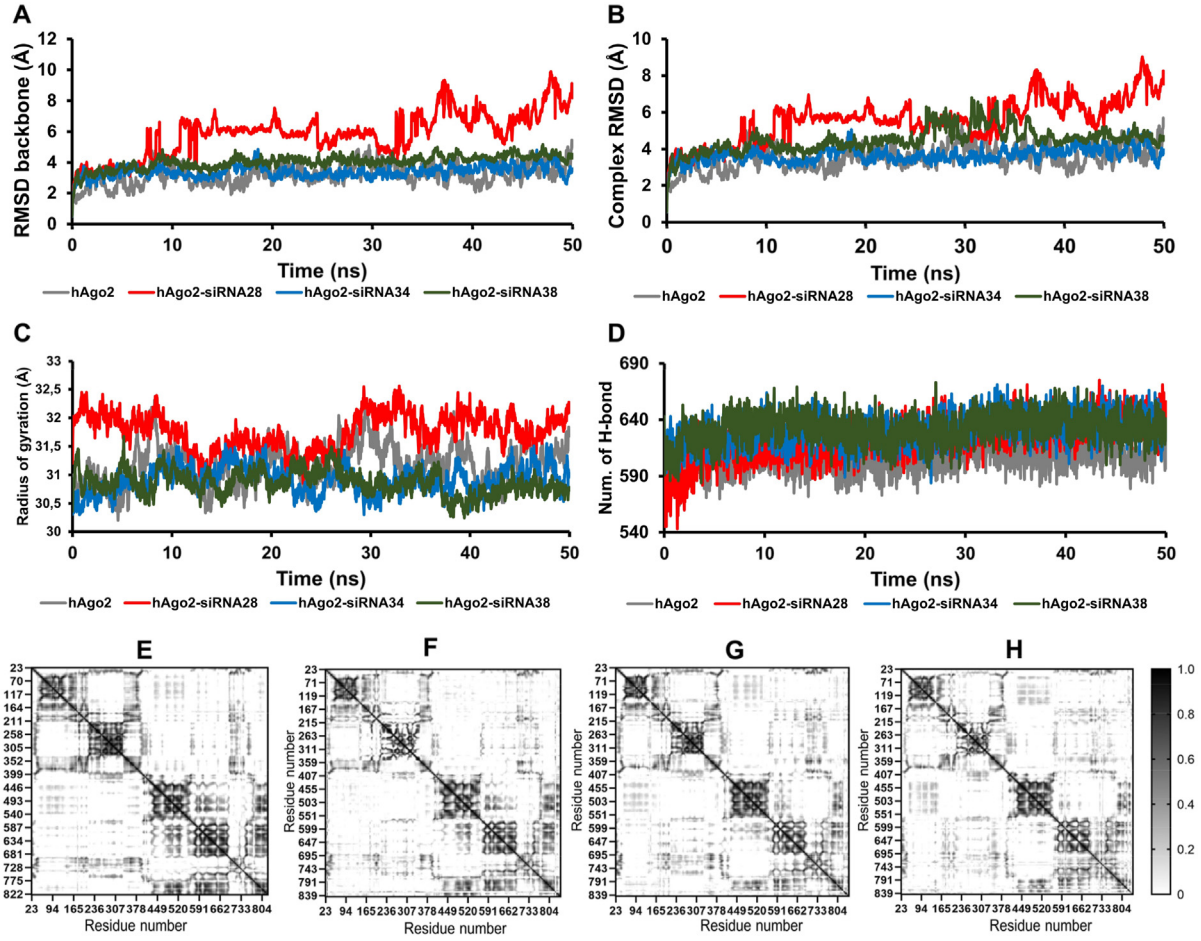

Fig. 6. Molecular dynamic of the hAgo2-siRNA complex. A) RMSD backbone, B) Complex RMSD, C) radius of gyration, number of hydrogen bond, E) DCCM of hAgo2, F) DCCM of hAgo2-siRNA 28, G) DCCM of hAgo2-siRNA 34, H) DCCM of hAgo2-siRNA 38.

4. Discussion

BRAF is a serine-threonine (Ser/Thr) protein kinase and a key component of the RAS/RAF/MEK/ERK signaling pathway. Upon activation by RAS, BRAF phosphorylates MEK, which subsequently activates ERK. This pathway plays a critical role in regulating cell proliferation, survival, and motility [23]. Mutations in BRAF are a primary driver of cancer cell formation, with the V600E mutation being the most frequently reported, accounting for approximately 80 % of all mutation cases. This mutation results in hyperactivation of BRAF kinase activity. Additionally, other mutations, such as V600D, V600K, and V600G, also contribute to increased BRAF activity [24]. Although the siRNA used in this study was designed based on the wild-type sequence, it remains effective in silencing mutant transcripts, particularly when mutations occur outside the siRNA binding region. This strategy enables suppression of both wild-type and mutant alleles, as previous studies have shown that point mutations in the siRNA target gene (CD46) did not affect silencing efficiency [25]. Various inhibitor compounds have been developed to suppress BRAF activity; however, many have failed due to resistance mechanisms, particularly BRAF amplification. BRAF amplification increases protein abundance and reduces the efficacy of inhibitors in blocking BRAF phosphorylation. Consequently, siRNA-based therapeutics are a promising approach for inhibiting BRAF expression.

This study predicted siRNA sequences targeting the BRAF gene by applying the Ui-Tei, Reynolds, and Amarzguioui guidelines. The Ui-Tei rules specify the presence of A/U at the 5′ end of the antisense strand, G/C at the 5′ end of the sense strand, at least five A/U residues in the 5′ terminal one-third of the antisense strand, and the absence of GC stretches exceeding nine nucleotides [26]. Reynolds identified key criteria for effective siRNA functionality, including low G/C content, low internal stability at the 3′-terminus of the sense strand, absence of inverted repeats, and specific base preferences at positions 3, 10, 13, and 19. Similarly, Amarzguioui's guidelines suggest that effective siRNAs have A/U at the terminal ends of the sequence and exclude U1 and G19 [27]. The selected siRNA sequences conform to these criteria, ensuring a melting temperature (Tm) above 20 °C, a range recommended for improved silencing efficiency [28]. This analysis identified seven potential siRNA candidates, which were subsequently validated using multiple parameters.

The seven potential siRNAs were validated based on GC content, heat capacity, and various prediction systems. The GC content significantly influences siRNA efficacy, with a negative correlation observed between GC content and siRNA functionality. siRNA targets with higher GC content are more prone to folding, potentially reducing target accessibility. Optimal siRNA effectiveness is generally associated with a GC content range of 30–52 % [29]. The calculated Tm(Cp) and Tm(Conc) values for the predicted siRNAs serve as indicators of their efficacy, with higher values suggesting enhanced silencing potential. Additionally, the seven siRNAs demonstrated favorable scores in siPRED, OligoWalk, and siExplorer prediction systems. According to siPRED, a predicted inhibition value of $\geq$70 % indicates high efficacy [16]. The OligoWalk system identifies siRNAs with a probability score of $\geq$0.7 as efficient [15] while the siExplorer system considers siRNAs with a score of $\geq$60 % as potential candidates [30]. The selected siRNAs also exhibited a low probability of self-folding and a high likelihood of binding to target mRNA. Further analysis of interactions between the siRNAs and hAgo2 is crucial to ensure their functionality and stability.

The human Argonaute2 protein (hAgo2) is structured into different regions: The N-terminal region along with Linker1 (1–225), the PAZ domain with Linker2 (226–449), the MID region (450–572), and the PIWI domains (573–859). It contains catalytic sites at D597, E637, D669, and H807, which are responsible for its silencing activity [31]. Short double-stranded siRNA molecules bind to the hAgo2 protein, where one strand, termed the guide strand, is selected and retained within the complex. Subsequently, the hAgo2-siRNA complex recruits additional proteins to assemble the RNA-induced silencing complex (RISC). The RISC specifically binds to complementary mRNA sequences, and hAgo2 mediates the cleavage of the target mRNA, leading to its degradation [32]. The results of molecular docking in this study showed that three siRNAs had the most negative binding affinity when interacting with hAgo2, namely siRNA 28, siRNA 34, and siRNA 38.

Then molecular dynamic simulation analyzes the stability of the hAgo2 structure, the siRNAs structure, and the hAgo2-siRNAs interaction. The structures of hAgo2 and siRNA tend to be stable during the simulation. During the 50 ns molecular dynamics simulation, siRNA 34 (5′-UUCCAAAUGCAUAUACAUCUG-3′) and siRNA 38 (5′-UUGUUGAUGUUUGAAUAAGG- U-3′) demonstrated a shift in their binding orientation on the hAgo2 protein. Specifically, both siRNAs repositioned such

that their 5′and 3′ends interacted with the MID and PAZ domains, respectively (Fig. 7). These results are reinforced by previous research which states that for effective gene silencing, the guide strand of siRNA must be correctly positioned within hAgo2, with its 5′ and 3′ termini anchored to the MID and PAZ domains, respectively. This interaction is essential for maintaining the structural conformation, stability, and catalytic activity of the RNA-induced silencing complex (RISC) [30].

In addition to identifying optimal siRNA candidates for BRAF silencing, this study offers a novel computational pipeline for predicting functionally effective siRNAs. Previous computational approaches have been employed to predict siRNAs targeting genes such as KRAS, as well as viral nucleocapsid proteins from Nipah virus and coronaviruses [30,33,34]. However, those studies did not explore the dynamic interactions between siRNA and human Argonaute 2 (hAgo2). In contrast, the present study examines this critical aspect by analyzing the positional shifts of siRNA 34 and siRNA 38 during their interaction with hAgo2, which contributes to their optimal functional performance. The siRNA–hAgo2 dynamic interaction is a key factor in determining whether an siRNA can effectively participate in gene silencing, and therefore, must be considered in functional siRNA design [35].

Previous research stated that the use of siRNA was very effective in inhibiting the expression of oncogene proteins. For instance, siRNA has been shown to more effectively suppress AKT expression compared to small molecule-based drugs in human glioblastoma cell lines [36]. Additionally, research has highlighted the efficacy of siRNA in targeting and inhibiting the KRAS oncogene [37]. This study identifies two siRNAs with the highest potential for silencing BRAF expression. Despite the remarkable effectiveness of siRNA in gene silencing, its application is limited by challenges such as low cellular uptake and susceptibility to degradation by nucleases. Consequently, the development of an appropriate delivery system is essential to maximize siRNA stability and therapeutic efficacy.

The use of siRNA as anticancer agent faced several limitations, including low cell membrane permeability and easily degraded by cytosolic nucleases [30]. Therefore, further research for siRNA delivery system is required. Several delivery systems have been proposed to enhance the efficacy of siRNA, including siRNA-ligand conjugates, lipid-based delivery systems, and siRNA-polymer bio conjugates. Among these, conjugating ligands directly to siRNA has emerged as a promising approach for improving delivery efficiency. Various ligands, such as small molecules, carbohydrates, aptamers, peptides, and antibodies, have been chemically attached to siRNA to enhance cellular uptake and facilitate specific cell targeting [38]. Additionally, liposomes have been extensively developed as drug delivery carriers, utilizing a variety of synthetic lipids. These liposomes not only protect siRNA from enzymatic degradation but also enable its efficient penetration through the cell membrane [39].

Polymers play a crucial role in enhancing the intracellular delivery of nucleic acids, including antisense oligonucleotides (ASOs) and plasmid DNA (pDNA). Cationic polymers facilitate nucleic acid condensation through electrostatic interactions, thereby improving cellular uptake. The precise chemical modification of polymeric nucleic acids enables the development of diverse nanostructures with tailored properties. Several polymer-based siRNA delivery systems have demonstrated therapeutic potential in clinical trial [40]. Further research is needed to determine the most suitable delivery system for siRNA 34 and siRNA 38.

5. Conclusions

This current study predicted the most potent siRNA for BRAF silencing, namely siRNA 34 and siRNA 38. These two siRNAs meet various parameters used in this study such as melting temperature, GC content, heat capacity, hairpin probability, ability to bind with target mRNA, and the interaction with hAgo2. This study also provides a comprehensive computational method for siRNA design so that the siRNA obtained is more effective. The low stability of siRNA necessitates an effective delivery method, highlighting the need for further research to identify the most suitable delivery system. Further research using cell lines or animal models is also necessary to validate the findings of this study.

Ethics information

As the research did not include experiments involving human participants or animal models, no ethical clearance or approval was required in accordance with institutional and journal guidelines.

Funding

This research did not receive financial support from any public, commercial, or nonprofit funding agencies.

Conflicts of interest

The authors stated that there is no potential conflict of interest in this study.

Acknowledgements

The authors gratefully acknowledge the HPC AI-Center at Universitas Brawijaya for providing computational resources to support the molecular dynamics simulations. The authors also thank Professor Widodo for granting access to the YASARA v23.4.25 software used in this study.

References

[1] N. Cope, C. Candelora, K. Wong, S. Kumar, H. Nan, M. Grasso, B. Novak, Y. Li, R. Marmorstein, Z. Wang, Mechanism of BRAF activation through biochemical characterization of the recombinant full-length protein, Chembiochem 19 (2018) 1988–1997, https://doi.org/10.1002/cbic.201800359.

[2] A. Zaman, W. Wu, T.G. Bivona, Targeting oncogenic BRAF: past, present, and future, Cancers 11 (2019) 1197, https://doi.org/10.3390/cancers11081197.

[3] H. Lavoie, M. Therrien, Regulation of RAF protein kinases in ERK signalling, Nat Rev Mol Cell Biol 16 (2015) 281–298, https://doi.org/10.1038/nrm3979.

[4] C.H. Johansson, S.E. Brage, BRAF inhibitors in cancer therapy, Pharmacol Ther 142 (2014) 176–182, https://doi.org/10.1016/j.pharmthera.2013.11.011.

[5] H. Yang, B. Higgins, K. Kolinsky, K. Packman, W.D. Bradley, R.J. Lee, K. Schostack, M.E. Simcox, S. Kopetz, D. Heimbrook, B. Lestini, G. Bollag, F. Su, Antitumor activity of BRAF inhibitor vemurafenib in preclinical models of BRAF-mutant colorectal cancer, Cancer Res 72 (2012) 779–789, https://doi.org/10.1158/0008-5472.CAN-11-2941.

[6] L. Yu, E. Favoino, Y. Wang, Y. Ma, X. Deng, X. Wang, The CSPG4-specific monoclonal antibody enhances and prolongs the effects of the BRAF inhibitor in melanoma cells, Immunol Res 50 (2011) 294–302, https://doi.org/10.1007/s12026-011-8232-z.

[7] D.B. Johnson, A.M. Menzies, L. Zimmer, Z. Eroglu, F. Ye, S. Zhao, H. Rizos, A. Sucker, R.A. Scolyer, R. Gutzmer, H. Gogas, R.F. Kefford, J.F. Thompson, J.C. Becker, C. Berking, F. Egberts, C. Loquai, S.M. Goldinger, G.M. Pupo, W. Hugo, X. Kong, L.A. Garraway, J.A. Sosman, A. Ribas, R.S. Lo, G.V. Long, D. Schadendorf, Acquired BRAF inhibitor resistance: a multicenter meta-analysis of the spectrum and frequencies, clinical behaviour, and phenotypic associations of resistance mechanisms, Eur J Cancer 51 (2015) 2792–2799, https://doi.org/10.1016/j.ejca.2015.08.022.

[8] J.L. Manzano, L. Layos, C. Bugés, M.D.L.L. Gil, L. Vila, E. Martínez-Balibrea, A. Martínez-Cardús, Resistant mechanisms to BRAF inhibitors in melanoma, Ann Transl Med 4 (2016), https://doi.org/10.21037/atm.2016.06.07, 237–237.

[9] S. Jain, K. Pathak, A. Vaidya, Molecular therapy using siRNA: recent trends and advances of multi target inhibition of cancer growth, Int J Biol Macromol 116 (2018) 880–892, https://doi.org/10.1016/j.ijbiomac.2018.05.077.

[10] S. Naghizadeh, A. Mohammadi, B. Baradaran, B. Mansoori, Overcoming multiple drug resistance in lung cancer using siRNA targeted therapy, Gene 714 (2019) 143972, https://doi.org/10.1016/j.gene.2019.143972.

[11] Q. Huang, L. Li, L. Li, H. Chen, Y. Dang, J. Zhang, N. Shao, H. Chang, Z. Zhou, C. Liu, B. He, H. Wei, J. Xiao, MDM2 knockdown mediated by a triazine-modified dendrimer in the treatment of non-small cell lung cancer, Oncotarget 7 (2016) 44013–44022, https://doi.org/10.18632/oncotarget.9768.

[12] X. Cheng, Y. Zhou, S. Xu, H. Yu, J. Wu, J. Bao, L. Zhang, Risk-stratified distant metastatic thyroid cancer with clinicopathological factors and BRAF/TERT promoter mutations, Clin Endocrinol Diabetes 131 (2023) 577–582, https://doi.org/10.1055/a-2177-1051.

[13] Y. Naito, J. Yoshimura, S. Morishita, K. Ui-Tei, siDirect 2.0: updated software for designing functional siRNA with reduced seed-dependent off-target effect, BMC Bioinf 10 (2009) 392, https://doi.org/10.1186/1471-2105-10-392.

[14] T. Katoh, T. Suzuki, Specific residues at every third position of siRNA shape its efficient RNAi activity, Nucleic Acids Res 35 (2007) e27, https://doi.org/10.1093/nar/gkl1120.

[15] Z.J. Lu, D.H. Mathews, OligoWalk: an online siRNA design tool utilizing hybridization thermodynamics, Nucleic Acids Res 36 (2008) W104–W108, https://doi.org/10.1093/nar/gkn250.

[16] W.-J. Pan, C.-W. Chen, Y.-W. Chu, siPRED: predicting siRNA efficacy using various characteristic methods, PLoS One 6 (2011) e27602, https://doi.org/10.1371/journal.pone.0027602.

[17] V.S. Ayyagari, Design of siRNA molecules for silencing of membrane glycoprotein, nucleocapsid phosphoprotein, and surface glycoprotein genes of SARS-CoV2, J Genet Eng Biotechnol 20 (2022) 65, https://doi.org/10.1186/s43141-022-00346-z.

[18] S. Bellaousov, J.S. Reuter, M.G. Seetin, D.H. Mathews, RNAstructure: web servers for RNA secondary structure prediction and analysis, Nucleic Acids Res 41 (2013) W471–W474, https://doi.org/10.1093/nar/gkt290.

[19] N.R. Markham, M. Zuker, DINAMelt web server for nucleic acid melting prediction, Nucleic Acids Res 33 (2005) W577–W581, https://doi.org/10.1093/nar/gki591.

[20] Y. Zhang, J. Wang, Y. Xiao, 3dRNA: 3D structure prediction from linear to circular RNAs, J Mol Biol 434 (2022) 167452, https://doi.org/10.1016/j.jmb.2022.167452.

[21] Y. Yan, H. Tao, J. He, S.-Y. Huang, The HDOCK server for integrated protein–protein docking, Nat Protoc 15 (2020) 1829–1852, https://doi.org/10.1038/s41596-020-0312-x.

[22] E. Krieger, G. Vriend, New ways to boost molecular dynamics simulations, J Comput Chem 36 (2015) 996–1007, https://doi.org/10.1002/jcc.23899.

[23] A. Marranci, Z. Jiang, M. Vitiello, E. Guzzolino, L. Comelli, S. Sarti, S. Lubrano, C. Franchin, I. Echevarría-Vargas, A. Tuccoli, A. Mercatanti, M. Evangelista, P. Sportoletti, G. Cozza, E. Luzi, E. Capobianco, J. Villanueva, G. Arrigoni, G. Signore, S. Rocchiccioli, L. Pitto, N. Tsinoremas, L. Poliseno, The landscape of BRAF transcript and protein variants in human cancer, Mol Cancer 16 (2017) 85, https://doi.org/10.1186/s12943-017-0645-4.

[24] I. Proietti, N. Skroza, N. Bernardini, E. Tolino, V. Balduzzi, A. Marchesiello, S. Michelini, S. Volpe, A. Mambrin, G. Mangino, G. Romeo, P. Maddalena, C. Rees, C. Potenza, Mechanisms of acquired BRAF inhibitor resistance in melanoma: a systematic review, Cancers 12 (2020) 2801, https://doi.org/10.3390/cancers12102801.

[25] Q. Du, A systematic analysis of the silencing effects of an active siRNA at all single-nucleotide mismatched target sites, Nucleic Acids Res 33 (2005) 1671–1677, https://doi.org/10.1093/nar/gki312.

[26] K. Ui-Tei, Guidelines for the selection of highly effective siRNA sequences for mammalian and chick RNA interference, Nucleic Acids Res 32 (2004) 936–948, https://doi.org/10.1093/nar/gkh247.

[27] M. Amarzguioui, H. Prydz, An algorithm for selection of functional siRNA sequences, Biochem Biophys Res Commun 316 (2004) 1050–1058, https://doi.org/10.1016/j.bbrc.2004.02.157.

[28] F. Safari, S.R. Barouji, A.M. Tamaddon, Strategies for improving siRNA-induced gene silencing efficiency, Adv Pharmaceut Bull 7 (2017) 603–609, https://doi.org/10.15171/apb.2017.072.

[29] A. Reynolds, D. Leake, Q. Boese, S. Scaringe, W.S. Marshall, A. Khvorova, Rational siRNA design for RNA interference, Nat Biotechnol 22 (2004) 326–330, https://doi.org/10.1038/nbt936.

[30] P.S. Ramalingam, S. Arumugam, Computational design and validation of effective siRNAs to silence oncogenic KRAS, 3 Biotech 13 (2023) 350, https://doi.org/10.1007/s13205-023-03767-w.

[31] Y. Kamiya, Y. Takeyama, T. Mizuno, F. Satoh, H. Asanuma, Investigation of strand-selective interaction of SNA-modified siRNA with AGO2-MID, Int J Mol Sci 21 (2020) 5218, https://doi.org/10.3390/ijms21155218.
[32] X. Ye, N. Huang, Y. Liu, Z. Paroo, C. Huerta, P. Li, S. Chen, Q. Liu, H. Zhang, Structure of C3PO and mechanism of human RISC activation, Nat Struct Mol Biol 18 (2011) 650–657, https://doi.org/10.1038/nsmb.2032.
[33] U.F. Chowdhury, M.U.S. Shohan, K.I. Hoque, M.A. Beg, M. K.S. Siam, M.A. Moni, A computational approach to design potential siRNA molecules as a prospective tool for silencing nucleocapsid phosphoprotein and surface glycoprotein gene of SARS-CoV-2, Genomics 113 (2021) 331–343, https://doi.org/10.1016/j.ygeno.2020.12.021.
[34] A. Mahfuz, M.A. Khan, E.H. Sajib, A. Deb, S. Mahmud, M. Hasan, O. Saha, A. Islam, M.M. Rahaman, Designing potential siRNA molecules for silencing the gene of the nucleocapsid protein of Nipah virus: a computational investigation, Infect Genet Evol 102 (2022) 105310, https://doi.org/10.1016/j.meegid.2022.105310.
[35] A. Alagia, A.F. Jorge, A. Aviñó, T.F.G.G. Cova, R. Crehuet, S. Grijalvo, A.A.C.C. Pais, R. Eritja, Exploring PAZ/3′-overhang interaction to improve siRNA specificity. A combined experimental and modeling study, Chem Sci 9 (2018) 2074–2086, https://doi.org/10.1039/C8SC00010G.
[36] Y. Cheng, X. Ren, Y. Zhang, R. Patel, A. Sharma, H. Wu, G.P. Robertson, L. Yan, E. Rubin, J.-M. Yang, eEF-2 kinase dictates cross-talk between autophagy and apoptosis induced by Akt inhibition, thereby modulating cytotoxicity of novel Akt inhibitor MK-2206, Cancer Res 71 (2011) 2654–2663, https://doi.org/10.1158/0008-5472.CAN-10-2889.
[37] M.J. Kim, S.J. Lee, J.H. Ryu, S.H. Kim, I.C. Kwon, T.M. Roberts, Combination of KRAS gene silencing and PI3K inhibition for ovarian cancer treatment, J Contr Release 318 (2020) 98–108, https://doi.org/10.1016/j.jconrel.2019.12.019.
[38] A.A. Turanov, A. Lo, M.R. Hassler, A. Makris, A. Ashar-Patel, J.F. Alterman, A.H. Coles, R.A. Haraszti, L. Roux, B.M.D.C. Godinho, D. Echeverria, S. Pears, J. Iliopoulos, R. Shanmugalingam, R. Ogle, Z.K. Zsengeller, A. Hennessy, S.A. Karumanchi, M.J. Moore, A. Khvorova, RNAi modulation of placental sFLT1 for the treatment of preeclampsia, Nat Biotechnol 36 (2018) 1164–1173, https://doi.org/10.1038/nbt.4297.
[39] T.M. Allen, P.R. Cullis, Liposomal drug delivery systems: from concept to clinical applications, Adv Drug Deliv Rev 65 (2013) 36–48, https://doi.org/10.1016/j.addr.2012.09.037.
[40] Y. Dong, D.J. Siegwart, D.G. Anderson, Strategies, design, and chemistry in siRNA delivery systems, Adv Drug Deliv Rev 144 (2019) 133–147, https://doi.org/10.1016/j.addr.2019.05.004.